

## FISSION TIME SCALES AND DISTRIBUTIONS STUDIED USING A LANGEVIN DYNAMICAL MODEL

 **Charmi Vadagama<sup>1\*</sup>, Pruthul Desai<sup>1</sup>, M.T. Senthil Kannan<sup>2</sup>**

<sup>1</sup>*Department of Physics, Sir P.T. Sarvajanic College of Science, Surat-395007, India*

<sup>2</sup>*Department of Physics, Christ the King Engineering College, Karamadai - 641104, India*

*\*Corresponding Author E-mail: [charmyl612@gmail.com](mailto:charmyl612@gmail.com)*

Received January 1, 2026; revised February 16, 2026; accepted February 18, 2026

The fission time scale and associated distributions play a crucial role in investigating the full dynamical evolution of the excited compound nucleus. In the present work, we have performed a one-dimensional Langevin dynamical model calculation to simulate the fission time scale and corresponding fission time distributions (FTDs) for <sup>125</sup>Cs, <sup>213</sup>Fr, and <sup>243</sup>Am. The time evolution of the collective deformation coordinate from the ground state to scission is followed under the influence of dissipation, fluctuations, and realistic fission barriers, and a large ensemble of trajectories is used to construct fission-time distributions for each compound nucleus. The results reveal distinct differences in the shapes and widths of the distributions, characterized by extended long-time components that significantly impact the average fission time. Particle evaporation is found to play an important role in shaping the fission time distributions by modifying the excitation energy during the dynamical evolution. These findings emphasize the importance of analyzing the full fission time distribution, rather than relying solely on average values, for a realistic description of fission dynamics.

**Keywords:** Nuclear fission; Fission time scale; Fission time distribution; Langevin dynamical model; Neutron multiplicities

**PACS:** 24.75.+i, 25.85.-w, 24.60.ky

### INTRODUCTION

Nuclear fission is a complex many-body process in which an excited compound nucleus evolves from its ground-state configuration to scission under the combined influence of the mean nuclear potential, dissipation, fluctuation, and statistical particle emission. It has been a topic of great interest and has been extensively studied both theoretically and experimentally [1-3]. Also, the study of nuclear fission dynamics is a challenging subject due to the intricate nature of this process. A compound nucleus may undergo fission depending on the excitation energy, angular momentum, fission barrier, and other factors. The dynamics of the fission process are governed primarily by the target-projectile combination, viz -a- viz., the total mass and the excitation energy. This relevance can be examined by using the fission timescale ( $\tau_f$ ), which is the time required for the CN to reach the scission configuration from the ground state shape. Significant effort has been made to comprehend fission timescales through various experimental techniques. Fission time ( $\tau_f$ ) of an excited compound nucleus can be inferred from the measured particle multiplicities such as pre-scission neutron multiplicities [4, 5], charged particles (proton and  $\alpha$ ) [6], and  $\gamma$ -rays [7]. Also, the average fission time ( $\tau_f$ ) can be estimated from observables such as the evaporation residue (ER) cross-section [8] and fission probabilities [9]. All these nuclear probes are considered indirect probes, and with a proper model, they are used to evaluate the fission time in the range of  $10^{-21}$ s ( $1 \text{ zs} = 10^{-21}$ s). On the other hand, direct probes, including crystal blocking and K-shell X-ray measurements, determine significantly longer lifetimes in the order of  $10^{-18}$ s (attosecond) scales. This apparent discrepancy has motivated renewed interest in dynamical approaches that explicitly follow the time evolution of the fissioning system, incorporating fluctuations, dissipation, and particle evaporation on an event-by-event basis. A one-dimensional Langevin dynamical model has been used recently to resolve this discrepancy [10]. In this work, a similar study is extended for a wide range of masses with different excitation energies.

### THEORETICAL MODEL

In the present work, a stochastic one-dimensional Langevin dynamical model is utilized to describe the full dynamical evolution of an excited compound nucleus, with the elongation of the nucleus considered as a collective coordinate and usually defined in terms of the Funny-Hill shape parameter  $c$  [11]. The one-dimensional Langevin equation in terms of  $c$  is given by,

$$\begin{aligned} \frac{dp}{dt} &= -\frac{p^2}{2} \frac{dm^{-1}(c)}{dc} - \frac{dF(c)}{dc} - \beta p + g\Gamma(t), \\ \frac{dc}{dt} &= \frac{p}{m(c)}, \end{aligned} \quad (1)$$

where  $c$  is the collective coordinate defining the deformation of a fissioning nucleus, and  $p$  is the collective momentum conjugate to  $c$ . The shape-dependent collective inertia  $m(c)$  is calculated by employing the Werner-Wheeler approximation [12] for the irrotational flow of incompressible nuclear fluid. The parameter  $\beta$  appearing in Eq. (1) is the

shape-independent reduced dissipation coefficient that represents the coupling between collective and intrinsic nuclear degrees of freedom and governs the irreversible energy flow from collective to the intrinsic excitation and is denoted by the ratio of the dissipation coefficient  $\eta$  to the inertia parameter  $m$  ( $\beta = \eta/m$ ). Since nuclear dissipation governs the fission time scale and the time available for prescission neutron emission, the prescission neutron multiplicity ( $\nu_{pre}$ ) is highly sensitive to  $\beta$ . Therefore,  $\beta$  is treated as the only adjustable parameter and is constrained by reproducing the experimental ( $\nu_{pre}$ ). The product  $g\Gamma(t)$  is the random force, with  $\Gamma(t)$  being the time-dependent stochastic part with time average  $\langle \Gamma(t) \rangle = 0$  and time-correlation  $\langle \Gamma(t)\Gamma(t') \rangle = \delta(t - t')$ .  $g$  is the strength of the random force, and it is related to the dissipation coefficient  $\eta$  through the fluctuation-dissipation theorem:  $g^2 = \eta T$  [13].

The driving force for the collective motion is extracted from the Helmholtz free energy:

$$F(c) = V(c) - \{a(c) - a_0\} T^2, \tag{2}$$

where  $V(c)$  and  $a(c)$  are the deformation-dependent potential energy and level density parameter, respectively.  $a_0$  is the value of  $a(c)$  at the spherical shape ( $c = 1$ ).

The shell correction in the level density parameter  $a(c)$  is incorporated using Ignatyuk's prescription [14]. The nuclear temperature  $T$  in the above Eq. (2) is calculated from the ground state excitation energy ( $E^*$ ) and the ground state level density parameter  $a_0$  by using the Fermi gas relation:  $T = \sqrt{E^*/a_0}$ . The deformation-dependent shell correction energy in  $V(c)$  is obtained by solving a two-centered Woods-Saxon mean field [15], followed by the application of Strutinsky's prescription [16].

A large number of Langevin trajectories, approximately  $10^6$ , are sampled to reduce statistical uncertainties. For each event, dynamics are followed numerically up to  $10^{-15}$ s with a time-step of  $10^{-25}$ s. At each time step, evaporation of light particles ( $n, p, \alpha$ ) and GDR  $\gamma$ -rays are sampled with the Monte-Carlo technique. The standard statistical model prescription is considered to calculate the widths for these evaporation channels. The initial collective coordinate is that of a spherical nucleus, and its initial momentum distribution follows from an equilibrated thermal system. A Langevin trajectory is judged as a scission when the neck radius reaches its critical value  $C_{sc} = 0.3R_0$ ; ( $R_0$  being the spherical nucleus radius). For each fission event, fission time is evaluated with associated neutron evaporation fission channels. If  $c_f^i$  is the fission time for the  $i^{\text{th}}$  fission event, then the average fission time is calculated as  $\langle c_f \rangle = \frac{\sum_{i=1}^{N_f} c_f^i}{N_f}$ , where,  $N_f$  is the total number of fission events.

### RESULTS AND DISCUSSION

The details of the reactions chosen for the present work are given in Table I. For each compound nucleus excitation energy ( $E^*$ ), the reduced dissipation coefficient ( $\beta$ ) – determined by accurately reproducing experimental prescission  $\nu_{pre}(\text{Exp})$  along with the average fission time  $\langle c_f \rangle$ , and barrier height ( $B_f$ ) are listed. These nuclei were chosen to provide a systematic comparison of fission dynamics across a wide range of masses.

**Table I:** Details of the reactions

CN	$E^*$ (MeV)	$\nu_{pre}$ (Exp)	$\nu_{pre}$ (Cal)	$\beta$ (MeV/h)	$\langle c_f \rangle$ zs	$B_f$ (MeV)	Ref.
$^{125}\text{Cs}$	241.78	$4.0 \pm 0.5$	4.0676	4	$1.45 \times 10^3$	34.64	[5]
$^{213}\text{Fr}$	72.19	$3.28 \pm 0.30$	3.30	5.5	$1.53 \times 10^4$	18.44	[17]
$^{243}\text{Am}$	54.1	$1.35 \pm 0.14$	1.4312	0.5	$3.28 \times 10^1$	7.50	[18]

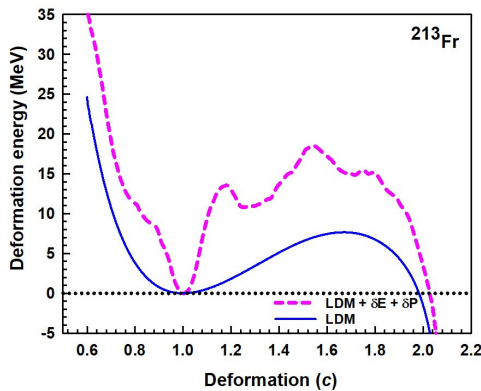
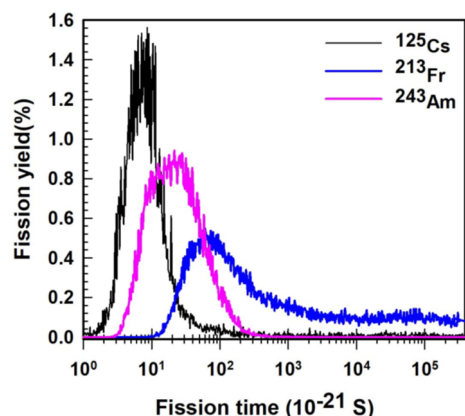


**Figure 1.** The Potential-energy landscape of the  $^{213}\text{Fr}$  nucleus calculated using the Liquid drop model (LDM) (solid line) and the LDM plus microscopic corrections (dashed line) as a function of the collective deformation coordinate  $c$

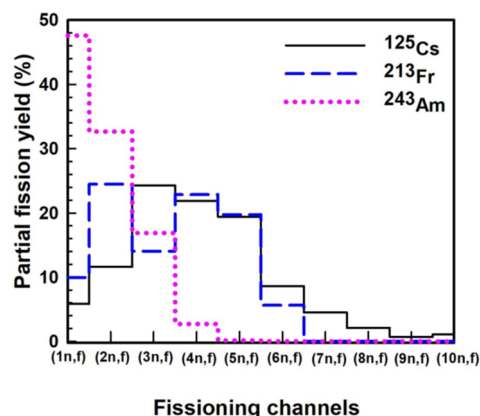
Fig. 1 shows the deformation energy landscape of  $^{213}\text{Fr}$  as a function of the deformation parameter  $c$ , incorporating shell and pairing corrections. The height and shape of the fission barrier play a crucial role in governing the fission dynamics by controlling both the barrier penetration probability and the residence time of the compound nucleus in the pre-scission region. The deformation-dependent microscopic corrections significantly modify the macroscopic LDM barrier, converting the originally single-humped fission barrier into a characteristic double-humped shape. This barrier structure leads to a competition between fission and particle evaporation, which strongly influences the average fission time and fission time distributions discussed below.

Fig. 2 depicts the total fission yields of  $^{125}\text{Cs}$ ,  $^{213}\text{Fr}$ , and  $^{243}\text{Am}$  as a function of fission time. The fission time distribution is sharply peaked at short times around  $10^{-20}$ s

with a very small non-vanishing tail up to  $10^5$  zs (zeptosecond) for the  $^{125}\text{Cs}$  compound system. Further, the distribution for  $^{213}\text{Fr}$  has a broader width with a peak around  $10^{-19}$ s, and has a considerably longer tail up to the maximum dynamical time. The pronounced long-time tail is correlated with the structured fission barrier of Fig. 1, where the second hump and the shallow intermediate minimum trap a non-negligible fraction of trajectories and allow for additional neutron evaporation before scission. Conversely, the actinide nucleus  $^{243}\text{Am}$  shows a narrower peak with a shorter  $\tau_f \sim 10^{-20}$  s without any long tail structure. From these distributions, we have observed the average fission time  $\langle\tau_f\rangle$ ,  $1.45 \times 10^3$  zs,  $1.53 \times 10^4$  zs and  $3.28 \times 10^1$  s for the systems  $^{125}\text{Cs}$ ,  $^{213}\text{Fr}$  and  $^{243}\text{Am}$ , respectively. The  $\langle\tau_f\rangle$  are mainly contributed by the long tail part of fission yields.



**Figure 2.** Fission yield distribution as a function of time for  $^{125}\text{Cs}$ ,  $^{213}\text{Fr}$ , and  $^{243}\text{Am}$



**Figure 3.** Partial fission yields from different isotopes of  $^{125}\text{Cs}$ ,  $^{213}\text{Fr}$ , and  $^{243}\text{Am}$  through neutron evaporation

Further, to understand the behaviour  $\tau_f$  more clearly, partial fission yields of different fission channels are depicted in Fig. 3. For  $^{125}\text{Cs}$ , fission channels up to  $(8n, f)$  have contributed, which indicates that the CN has survived for a longer dynamical time after the last particle evaporated. This behavior is consistent with the relatively higher fission barrier of  $^{125}\text{Cs}$ , which hinders early saddle crossing and allows successive neutron evaporations to occur. Since each neutron usually reduces the CN excitation by 8 to 10 MeV (separation energy kinetic energy), it makes the fission process slower. The same scenario is valid for  $^{213}\text{Fr}$  up to  $(6n, f)$  fission channel. For this system, the available  $E^*$  falls between 15 – 25 MeV, hence a substantial percentage of CN persists for a longer time. In contrast, a larger partial fission yield is observed for the  $(1n, f)$  and  $(2n, f)$  channels for  $^{243}\text{Am}$ , resulting in a very short fission timescale. Also, this behavior can be directly related to the comparatively lower fission barrier of  $^{243}\text{Am}$ , which allows rapid saddle crossing and suppresses higher-order evaporation chains.

## CONCLUSIONS

The present Langevin dynamical study demonstrates that the fission decay of the compound systems  $^{125}\text{Cs}$ ,  $^{213}\text{Fr}$ , and  $^{243}\text{Am}$  is governed by a subtle interplay between excitation energy, fission barrier structure, and dissipation strength. From this study, we conclude that the fission timescale primarily depends on CN mass, which determines the potential energy surface (PES). Consequently, the fission timescale of each nucleus is determined by the shape of the PES near the ground state configuration.

## ORCID

©Charmi Vadagama, <https://orcid.org/0009-0001-4603-8616>

## REFERENCES

- [1] G. Mohanto, M. T. Senthil Kannan, J. Sadhukhan, and B. Srinivasan, Phys. Rev. C, **110**, 034604 (2024). <https://doi.org/10.1103/PhysRevC.110.034604>
- [2] P. Fröbrich, and I. Gontchar, Phys. Rep. **292**, 131 (1998). [https://doi.org/10.1016/S0370-1573\(97\)00042-2](https://doi.org/10.1016/S0370-1573(97)00042-2)
- [3] Y. Jia, and J.-D. Bao, Phys. Rev. C, **75**, 034601 (2007). <https://doi.org/10.1103/PhysRevC.75.034601>
- [4] K. Kapoor, S. Verma, P. Sharma, R. Mahajan, N. Kaur, G. Kaur, B. Behera, *et al.*, Phys. Rev. C, **96**, 054605 (2017). <https://doi.org/10.1103/PhysRevC.96.054605>
- [5] D. Hinde, D. Hilscher, H. Rossner, B. Gebauer, M. Lehmann, and M. Wilpert, Phys. Rev. C, **45**, 1229 (1992). <https://doi.org/10.1103/PhysRevC.45.1229>
- [6] K. Ramachandran, A. Chatterjee, A. Navin, K. Mahata, A. Shrivastava, V. Tripathi, *et al.*, Pramana, **85**, 335 (2015). <https://doi.org/10.1007/s12043-015-0988-6>
- [7] P. Paul, Nucl. Phys. A, **569**, 73 (1994). [https://doi.org/10.1016/0375-9474\(94\)90097-3](https://doi.org/10.1016/0375-9474(94)90097-3)
- [8] B. B. Back, D. J. Blumenthal, *et al.*, Phys. Rev. C, **60**, 044602 (1999). <https://doi.org/10.1103/PhysRevC.60.044602>
- [9] V. Tishchenko, C.-M. Herbach, D. Hilscher, U. Jahnke, J. Galin, F. Goldenbaum, *et al.*, Phys. Rev. Lett. **95**, 162701 (2005). <https://doi.org/10.1103/PhysRevLett.95.162701>
- [10] M. T. Senthil Kannan, *et al.*, Phys. Rev. C, **98**, 021601 (2018). <https://doi.org/10.1103/PhysRevC.98.021601>

- [11] M. Brack, J. Damgaard, A.S. Jensen, H.C. Pauli, V.M. Strutinsky, and C.Y. Wong, *Rev. Mod. Phys.* **44**, 320 (1972). <https://doi.org/10.1103/RevModPhys.44.320>
- [12] J. R. Nix, *Nucl. Phys. A*, **130**, 241 (1969). [https://doi.org/10.1016/0375-9474\(69\)90730-1](https://doi.org/10.1016/0375-9474(69)90730-1)
- [13] Y. Abe, S. Ayik, P.-G. Reinhard, and E. Suraud, *Phys. Rep.* **275**, 49 (1996). [https://doi.org/10.1016/0370-1573\(96\)00003-8](https://doi.org/10.1016/0370-1573(96)00003-8)
- [14] A. Ignatyuk, M. Itkis, V. Okolovich, G. Smirenkin, and A. Tishin, *Sov. J. Nucl. Phys.* **21**, 255 (1975).
- [15] F. Garcia, O. Rodriguez, J. Mesa, J.D.T. Arruda-Neto, V.P. Likhachev, E. Garrote, *et al.*, *Comput. Phys. Commun.* **120**, 57 (1999). [https://doi.org/10.1016/S0010-4655\(99\)00199-X](https://doi.org/10.1016/S0010-4655(99)00199-X)
- [16] V.M. Strutinsky, *Nucl. Phys. A*, **122**, 1 (1968). [https://doi.org/10.1016/0375-9474\(68\)90699-4](https://doi.org/10.1016/0375-9474(68)90699-4)
- [17] J.O. Newton, D.J. Hinde, R.J. Charity, J.R. Leigh, J. Bokhorst, *et al.*, *Nucl. Phys. A*, **483**, 126 (1988). [https://doi.org/10.1016/0375-9474\(88\)90068-1](https://doi.org/10.1016/0375-9474(88)90068-1)
- [18] A. Saxena, *et al.*, *Phys. Rev. C*, **49**, 932 (1994). <https://doi.org/10.1103/PhysRevC.49.932>

#### МАСШТАБИ ТА РОЗПОДІЛИ ЧАСУ ПОДІЛУ, ДОСЛІДЖЕНІ З ЗАСТОСУВАННЯМ ДИНАМІЧНОЇ МОДЕЛІ ЛАНЖЕВЕНА

Чармі Вадагама<sup>1</sup>, Пругул Десаї<sup>1</sup>, М.Т. Сентіл Каннан<sup>2</sup>

<sup>1</sup>Кафедра фізики, коледж наук ім. сера П.Т. Сарваджаніка, Сурат-395007, Індія

<sup>2</sup>Кафедра фізики, інженерний коледж Христа Царя, Караматай - 641104, Індія

Шкала часу поділу та пов'язані з нею розподіли відіграють вирішальну роль у дослідженні повної динамічної еволюції збудженого складного ядра. У цій роботі ми виконали розрахунок одновимірної динамічної моделі Ланжевена для моделювання шкали часу поділу та відповідних розподілів часу поділу (FTD) для  $^{125}\text{Cs}$ ,  $^{213}\text{Fr}$  та  $^{243}\text{Am}$ . Часова еволюція колективної координати деформації від основного стану до розриву відстежується під впливом дисипації, флуктуацій та реалістичних бар'єрів поділу, а для побудови розподілів часу поділу для кожного складного ядра використовується великий ансамбль траєкторій. Результати показують чіткі відмінності у формах та ширині розподілів, що характеризуються протяжними довгочасовими компонентами, які суттєво впливають на середній час поділу. Виявлено, що випаровування частинок відіграє важливу роль у формуванні розподілу часу поділу, змінюючи енергію збудження під час динамічної еволюції. Ці результати підкреслюють важливість аналізу повного розподілу часу поділу, а не покладатися виключно на середні значення, для реалістичного опису динаміки поділу.

**Ключові слова:** ядерний поділ; шкала часу поділу; розподіл часу поділу; динамічна модель Ланжевена; нейтронні множинності